Carbonitriding Reduction of TiO_2 in the CH_4-H_2-N_2 System: Reduction Temperature Effect and Kinetics

R. Zhang [a], G.-Q. Fan [a,b*], Y. Hou [a], Y. You [a], J. Dang [a**]

[a] College of Materials Science and Engineering, Chongqing University, Chongqing, PR China
[b] Chongqing Key Laboratory of High Performance Oriented Electrical Steel, Chongqing Wangbian Electric (Group) Corp., Ltd., Chongqing, PR China
Corresponding author:**Gangqiang Fan: fangangqiang@cqwbdq.com; *Jie Dang: jiedang@cqu.edu.cn

(Received 27 November 2023; Accepted 27 May 2024)

Abstract

Understanding of the reaction kinetics can provide valuable information for the design and optimization of a reaction process. In this study, the reduction degree and carbonitriding ratio of TiO_2 in the CH_4-H_2-N_2 system were investigated to understand the carbonitriding reduction kinetics. The experimental results revealed the following key findings. The reduction degree of TiO_2 showed a significant increase within the temperature range of 1000 ºC to 1200 ºC. Simultaneously, the complete carbonitride time decreased as the temperature increased. However, it was observed that excessively high temperatures (1200 °C) had a detrimental effect on the reduction degree. Consequently, the optimal reduction temperature was determined to be 1100 °C, enabling a balance between reduction degree and reaction time. The carbonitriding reduction process of TiO_2 in the CH_4-H_2-N_2 system exhibited conformity with the unreacted nuclear model, with chemical reactions primarily controlling the process. A calculated apparent activation energy of 99.35 kJ/mol was obtained for the carbonitriding reduction process. The identification of the optimal reduction temperature and the dominant role of chemical reactions offer valuable insights for the design and optimization of carbonitriding processes involving titanium compounds.

Keywords: Ti(C, N, O); TiO_2; kinetics; CH_4-H_2-N_2 gas mixture

1.Introduction

Titanium, as a very active lithophile element, is widely distributed in the crust and lithosphere in the form of oxides[1, 2]. Titanium dioxide is the main oxide of titanium (commonly known as titanium white), which is widely used in chemical, textile, medical, food and other fields[3]. Meanwhile, as the end product of smelting most titanium-bearing minerals, TiO_2 is also an important raw material for the production of other titanium products.

Titanium carbides and nitrides, as advanced engineering ceramics, are widely used in coating materials, medical instruments, aerospace parts and other fields, while their solid solutions Ti(C, N) have similar excellent properties such as high hardness, high wear resistance, high chemical stability, high oxidation resistance, and high thermal conductivity[4-6]. Ti(C, N) can be used as metal-based ceramics and coating material, as well as a potential raw material (soluble anode) for electrolytic production of titanium sponge[7-9]. There are many production methods for titanium carbonitride, and the specific method varies depending on its intended use. At present, the main preparation process of powder titanium carbonitride includes carbothermic nitride, high temperature diffusion, high temperature nitride and so on[10-12], while the main preparation process of titanium carbonitride for coating includes ion plating, magnetron sputtering and vapor deposition[13-15]. Titanium dioxide is the main raw material for industrial production of titanium carbonitride by carbothermic nitride. TiO_2 powder and carbon powder were used as raw materials to generate titanium carbonitride powder by carbothermal reduction at a high temperature and in nitrogen atmosphere. The high production costs of titanium carbonitride, such as high reaction temperature, long reaction time, and expensive raw materials, pose challenges for its widespread application.

In recent years, hydrogen metallurgy, as a green and low emission smelting process, has attracted the attention of researchers, while hydrogen energy is also regarded as a green renewable energy with the greatest development potential in the 21st century[16-18]. As a typical hydrogen energy resource, methane gas has been shown to reduce metal oxides, such as MnO and NiO, at lower temperatures[19-22]. Zhang's group conducted a reduction study of titanium-bearing minerals using CH_4-H_2-Ar mixture and confirmed that titanium dioxide can be reduced to titanium oxycarbide at 1300 °C[23, 24]. And our team also have proposed the CH_4-H_2/CH_4-H_2-N_2 gas mixture reduction method, which proves that titanium-bearing minerals can be reduced and carbonized at a low temperature compared with the commercial process[2, 25-29]. Meanwhile, the previous experiments also confirmed that adding N_2 to the reduction gas containing methane could further reduce the reduction temperature and promote the reaction rate.

However, the kinetics of the reduction of TiO_2 in the CH_4-H_2-N_2 system remains unclear at present. Reaction kinetics plays a crucial role in the design of reactors and the selection of reaction parameters in practical production. Building upon our previous work[28], in which the synthesis of Ti(C, N, O), reaction mechanism, and the composition of the product have been investigated, we conducted investigations into the effects of time and temperature on the reduction rate and degree. Furthermore, we discussed the reduction kinetics and calculated the activation energy of the reduction

reaction. Based on the experimental results, we also explored the reduction mechanism of TiO_2 in the CH_4-H_2-N_2 system.

2.Experimental

2.1. Materials

The TiO_2 and Fe_2O_3 powders used in the present work are both analytical reagent with 99% purity (Chengdu Kelong Corporation, China). The CH_4, H_2 and N_2 gases employed in this study are all with 99.999% purity (Chongqing Ruike Corporation, China).

2.2 Experimental procedure

TiO_2 and Fe_2O_3 powders were mixed in a certain proportion, and then dried at 200 ºC for more than 12h to remove the water in the raw materials. Around 0.5g mixed powders were loaded in a corundum crucible (diameter 30 mm, height 5 mm), and then placed inside the vertical tube furnace. The furnace was first heated to the desired temperature in flowing N_2 at a rate of 10 ºC /min, while the flow rate of gas was controlled by gas flow controllers (Alicat, Model MC- 500SCCM-D, and MC-1SLPM-D). And then CH_4-N_2-H_2 gas mixture was introduced into the furnace from the top at a rate of 500 sccm/min. The experimental apparatus employed in this study has been described elsewhere[2].

3.Result and Discussion

3.1 The reaction sequence at different temperatures

In our previous studies, the phase transition process of TiO_2 during the reduction process at different temperatures has been studied. However, the obtained research data did not provide sufficient detail for the study of kinetics. In order to address this gap, a more comprehensive experimental study was carried out on the phase transition process of TiO_2 with adding 10 *wt.*% Fe_2O_3 at 1000 ºC, 1100 ºC and 1200 ºC based on our previous research. The reason for adding 10 wt.% Fe_2O_3 is that its reduction product metal iron will act as a catalyst in the following reductions, including methane pyrolysis[30], water-gas shift reaction[31], and Boudouard reaction[32], which is beneficial to reduction of TiO_2.

Figure 1 shows the XRD patterns of samples reduced at 1000 ºC for different time. It can be found that a large amount of TiO_2 was converted to Magnéli phase in the first ten minutes of reaction, while all the iron oxide in the sample was reduced to metallic iron. With the reduction time increasing to 20 minutes, a large amount of Ti_3O_5 and Ti_2O_3 was generated in the sample, accompanied by the disappearance of Magnéli phase. Meanwhile, the generation of Ti(C, N, O) can be also found in the sample, indicating that TiO_2 could be reduced to Ti(C, N, O) by CH_4-N_2-H_2 gas mixture at 1000 ℃. With the prolongation of reduction time, the Ti_2O_3 phase in the sample increased significantly, while the Ti_3O_5 phase decreased significantly. However, there were still a large amount of Ti_3O_5 and Ti_2O_3 in the samples after 90 minutes of reduction. It indicates that the carbonitriding rate of the sample was relatively slow at 1000℃. In addition, deposited carbon has been formed in the sample after 30 minutes of reduction, indicating that the pyrolysis rate of methane at this time has been greater than the

carbonitriding rate of the sample.

Meanwhile, in order to make more intuitive statistics of the phase transformation of the samples, X'pert Highscore software was used to Rietveld refine the XRD patterns, which can semi-quantitatively analyze the phase composition of the reduced sample. **Figure 2** shows the final fitting patterns of the Rietveld refinement, and the relevant quantitative analysis results are shown in **Table 1** (eliminating the presence of deposited carbon). In the case of samples with a single phase composition, the X'pert Highscore software requirements for rietveld refinement are a goodness of fit (R_{wp}) of less than 2% and an R-factor of fit (GOF) of less than 10%, which means that the results obtained are plausible. R_{wp} and GOF are both shown in the corresponding diffractogram in **Figure 2**, which are basically in accordance with the requirements. The results in **Table 1** eliminated the presence of deposited carbon for a more intuitive comparison.

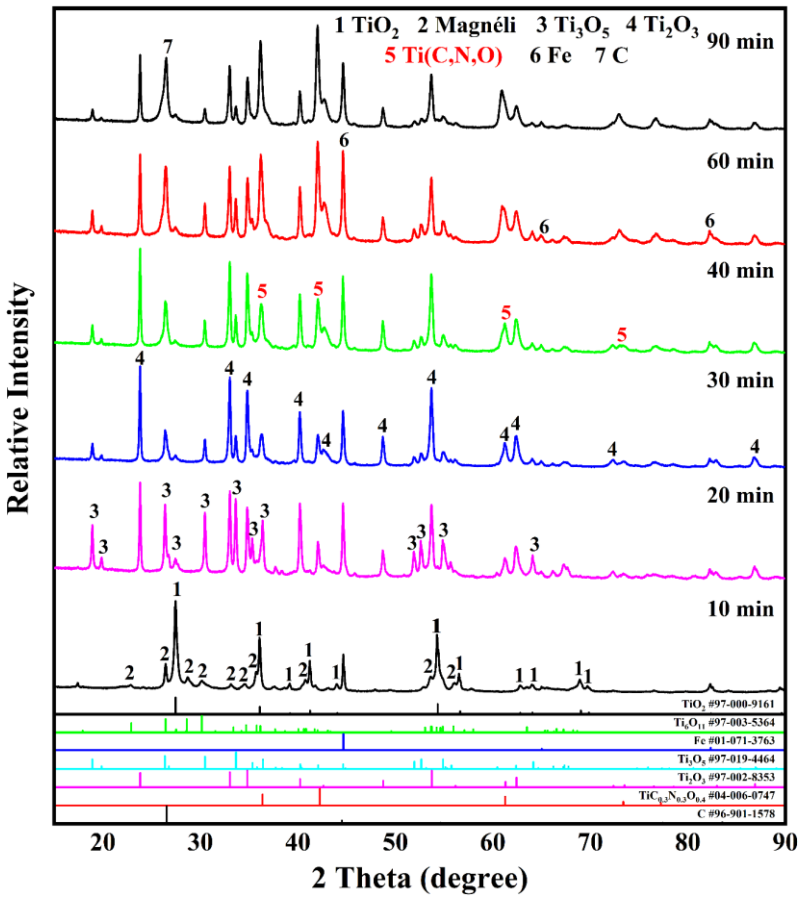

Figure 1 XRD patterns of TiO_2 - 10 *wt.*% Fe_2O_3 reduced at 1000 ℃ for different time

As shown in **Table 1**, the first 10 minutes of reaction are mainly the reduction of ferric oxide, while about half of the TiO_2 was converted to Magnéli phase. With the prolongation of reduction time, TiO_2 was rapidly reduced to Magnéli phase, while the Magnéli phase was first reduced to Ti_3O_5, then to Ti_2O_3, and final to Ti(C, N, O). Ti_3O_5 and Ti_2O_3 increased first and then decreased in the sample, while the Ti(C, N, O) was constantly being formed. However, there were still a large amount of low titanium oxides (Ti_3O_5 and Ti_2O_3) in the samples after 90 minutes of reduction, and the ratio of

Ti(C, N, O) in the sample was only 37.6 wt.%.

Figure 3 illustrates the XRD patterns of samples reduced at 1100 ºC for different time. It can be found that there has been obvious Ti (C, N, O) formation after reduction for 10 minutes, while the main phases of the sample are TiO_2, Ti_3O_5, Ti(C, N, O) and Fe. After 40 minutes of reduction, almost all TiO_2 in the sample has been reduced to Ti(C, N, O), with only trace amounts of TiO_2 and Ti_2O_3 remaining. It indicates that TiO_2 can be rapidly carbonitrided to Ti(C, N, O) at 1100 ºC. The content of Ti_2O_3 in the sample is almost non-existent throughout the reduction process, indicating that the increase of temperature will greatly promote the reduction rate of Ti_2O_3 to Ti(C, N, O), which is consistent with previous studies[28]. It is worth noting that the deposited carbon was already produced in the early stages of the reaction, which increased significantly with the increase of reduction time.

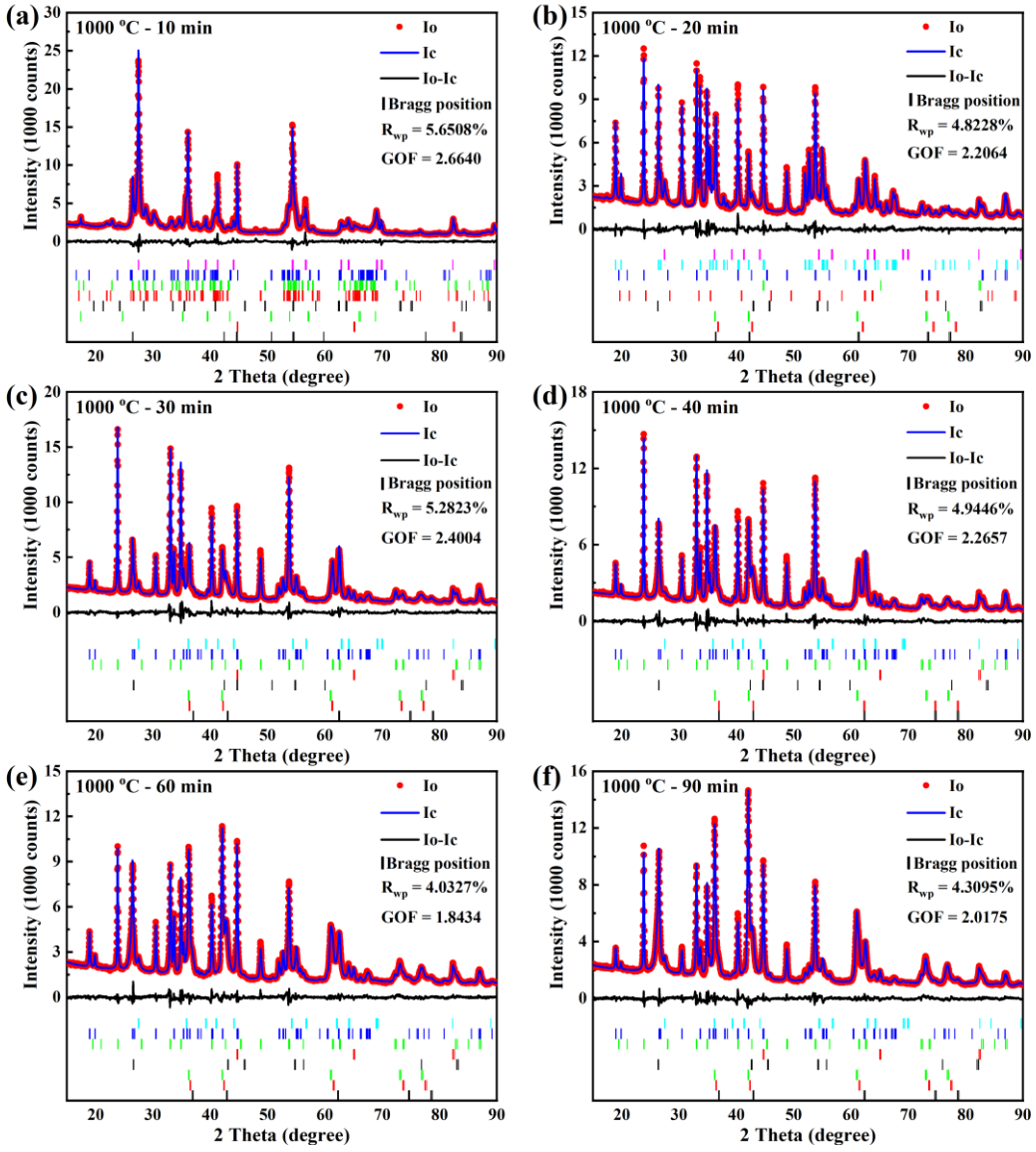

Figure 2 Final fitting patterns of the Rietveld refinement with the calculated XRD patterns of TiO_2 - 10 *wt.*% Fe_2O_3 reduced at 1000 ℃ for different time: (a) 10 min; (b) 20 min; (c) 30 min; (d) 40 min; (e) 60 min; (f) 90 min. Red dots (Io) are raw plots, blue lines (Ic) are calculated plots, and

black lines (Io-Ic) represent fitted lines.

Table 1 Phase content of TiO_2 - 10 *wt.*% Fe_2O_3 reduced at 1000 ℃ for different time (*wt.*%)

Time (min)	TiO_2	Magnéli	Ti_3O_5	Ti_2O_3	Ti(C, N, O)	Fe
10	44.72	50.56	-	1.44	-	3.18
20	8.63	-	50.73	31.87	5.56	3.21
30	4.27	-	28.04	49.95	14.13	3.61
40	6.97	-	23.45	41.59	23.01	4.98
60	5.44	-	23.29	30.40	35.29	5.58
90	3.94	-	19.29	32.48	37.60	6.69

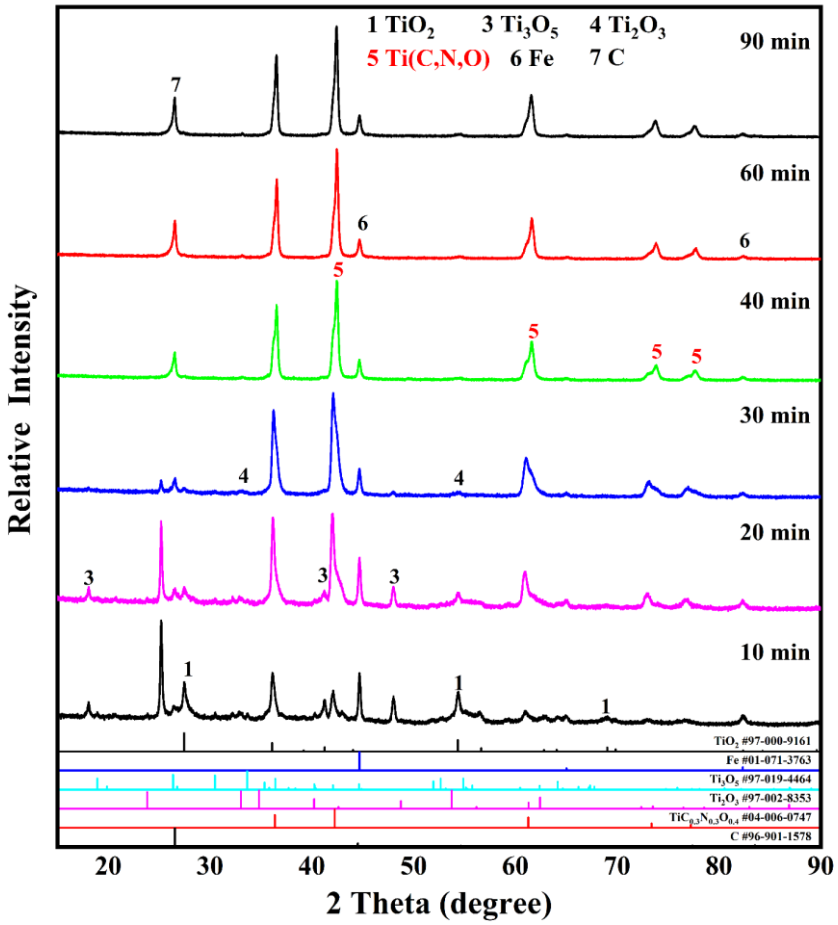

Figure 3 XRD patterns of TiO_2 - 10 *wt.*% Fe_2O_3 reduced at 1100 ℃ for different time

As shown in **Figure 4** and **Table 2**, the original X-ray diffraction patterns and Rietveld refinement patterns are in good agreement for all samples. About 15.03 wt.% Ti(C, N, O) was formed in the sample after 10 minutes of reduction, which was much better than the reduction result at 1000 ℃. With the reduction time increasing to 40 minutes, the content of Ti(C, N, O) in the sample exceeded 90 wt.%. This means that the carbonitriding process was basically complete. However, trace amount of TiO_2 and Ti_2O_3 still remained in the samples as the reduction time continued to extend. It is preliminarily inferred that this was caused by the poor kinetic conditions of the sample

at the bottom of the crucible.

Table 2 Phase content of TiO_2 - 10 *wt.*% Fe_2O_3 reduced at 1100 °C for different time (*wt.*%)

Time (min)	TiO_2	Ti_3O_5	Ti_2O_3	Ti(C, N, O)	Fe
10	32.60	43.09	4.97	15.03	4.31
20	19.85	26.89	0.95	47.69	4.62
30	6.19	5.98	3.20	80.62	4.02
40	2.02	-	2.02	90.98	4.99
60	1.38	-	1.49	91.38	5.75
90	1.05	-	0.87	91.99	6.09

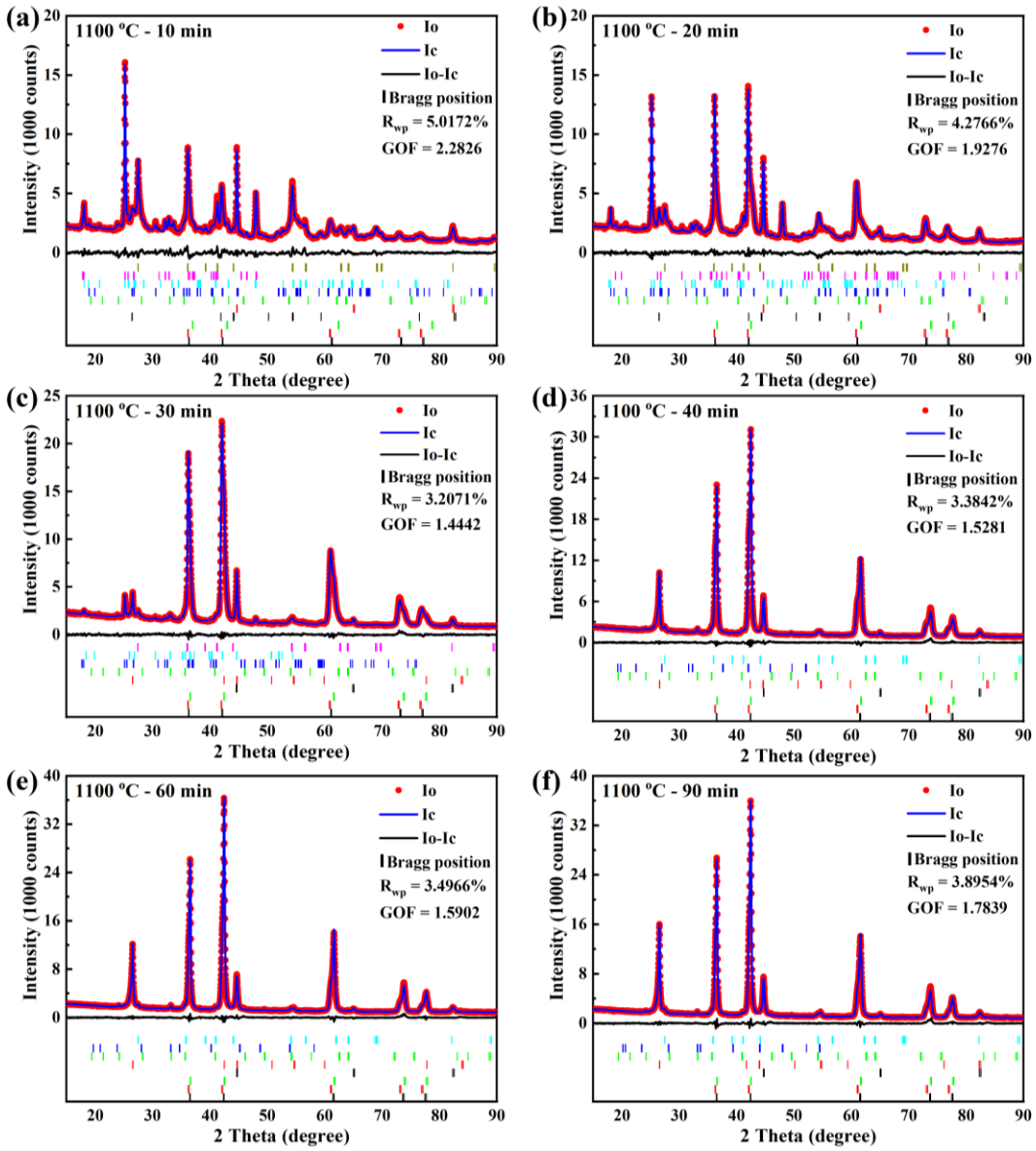

Figure 4 Final fitting patterns of the Rietveld refinement with the calculated XRD patterns of TiO_2 - 10 *wt.*% Fe_2O_3 reduced at 1100 °C for different time: (a) 10 min; (b) 20 min; (c) 30 min; (d) 40 min; (e) 60 min; (f) 90 min.

Furthermore, the XRD patterns and Rietveld refinement patterns of samples reduced at 1200°C for different durations are presented in **Figures 5** and **6**, respectively. The corresponding quantitative analysis results are summarized in **Table 3**. It is evident that nearly all of the TiO_2 in the sample underwent carbonitridation after a reaction time of 30 minutes. Carbon deposition occurred in the early stages of the reaction, but its production was significantly lower than that at 1100 °C, suggesting that the increase of temperature has a greater promotion effect on the reduction rate than on the methane pyrolysis reaction.

However, residual traces of TiO_2 and Ti_2O_3 are still observed in the samples as the reduction time is prolonged, which is consistent with the observations at 1100 °C.

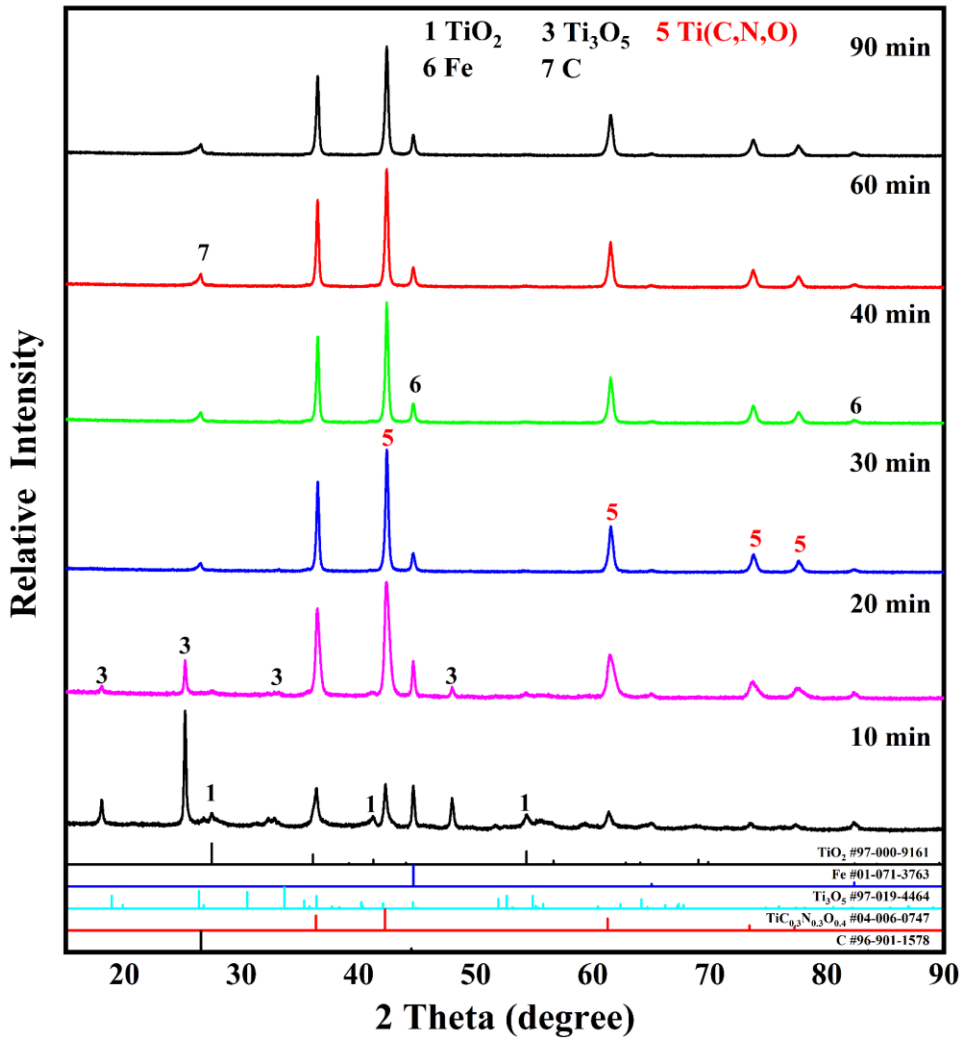

Figure 5 XRD patterns of TiO_2 - 10 *wt.*% Fe_2O_3 reduced at 1200 °C for different time

The morphologies of samples reduced at three temperatures for different time are shown in **Figure 7**. It can be seen that with the progress of the reaction, the microstructure of the solid material has a great change. The powder samples used in this study are easy to form clusters due to its small particle size and high specific surface area. At the early stage of reduction at 1000 ºC, TiO_2 was reduced to a low valent oxide

of titanium, and the particles change from dense to porous coral, while the surface is very smooth. With the subsequent generation of Ti(C, N, O), the surface of the porous coral-like sample becomes rough, while some small granular phases are formed. When the reduction temperature is increased, the sample is sintered at the early stage of reduction.

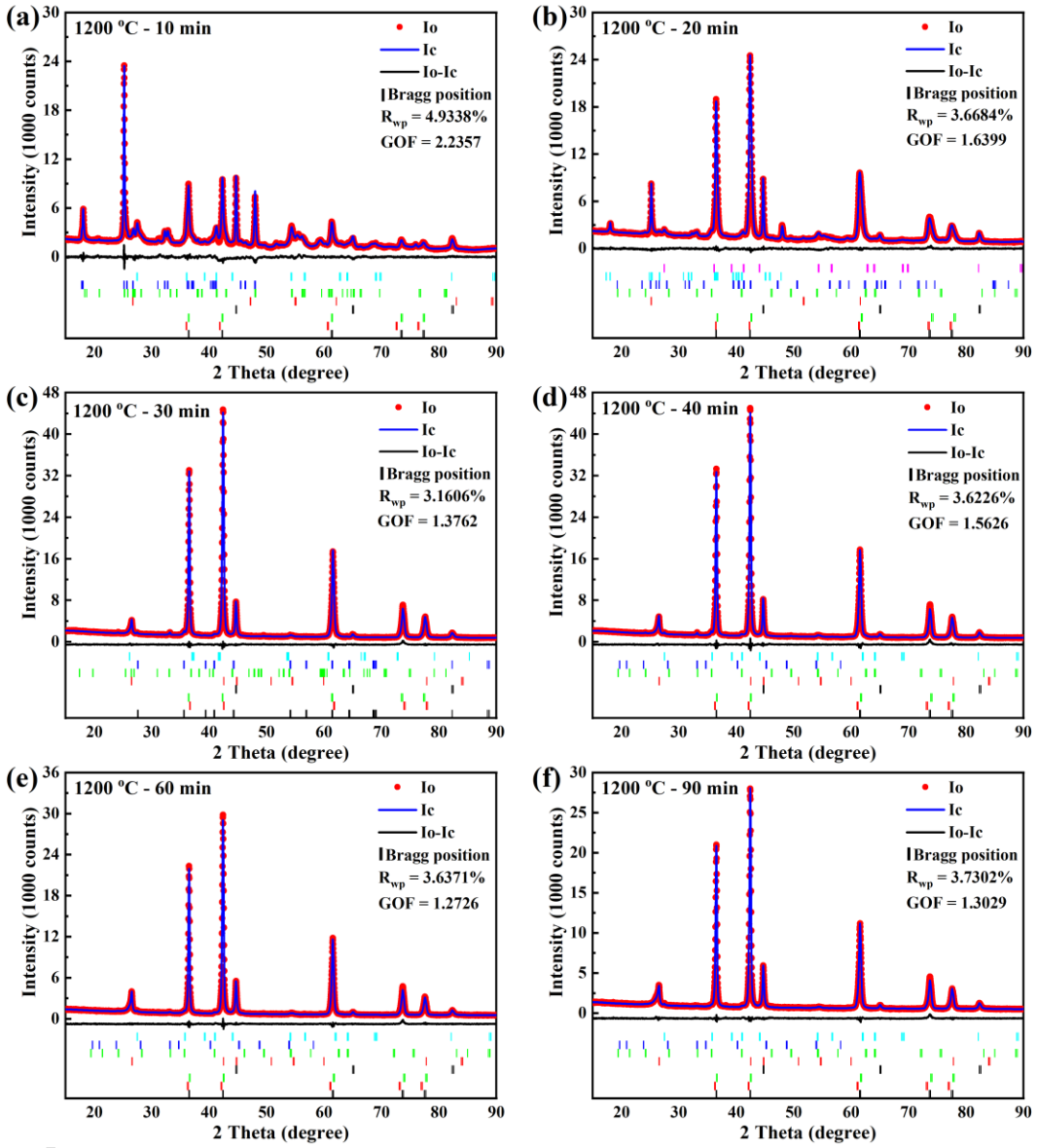

Figure 6 Final fitting patterns of the Rietveld refinement with the calculated XRD patterns of TiO_2 - 10 *wt.*% Fe_2O_3 reduced at 1200 ℃ for different time: (a) 10 min; (b) 20 min; (c) 30 min; (d) 40 min; (e) 60 min; (f) 90 min.

Table 3 Phase content of the TiO_2 - 10 *wt.*% Fe_2O_3 reduced at 1200 ℃ for different time (*wt.*%)

Time（min）	TiO_2	Ti_3O_5	Ti_2O_3	Ti(C, N, O)	Fe
10	26.89	43.28	2.94	21.22	5.67
20	6.14	12.89	2.42	73.62	4.93
30	1.04	-	1.77	91.35	5.84

40	1.02	-	2.05	90.76	6.17
60	0.73	-	1.25	91.25	6.77
90	0.75	-	0.43	91.80	7.02

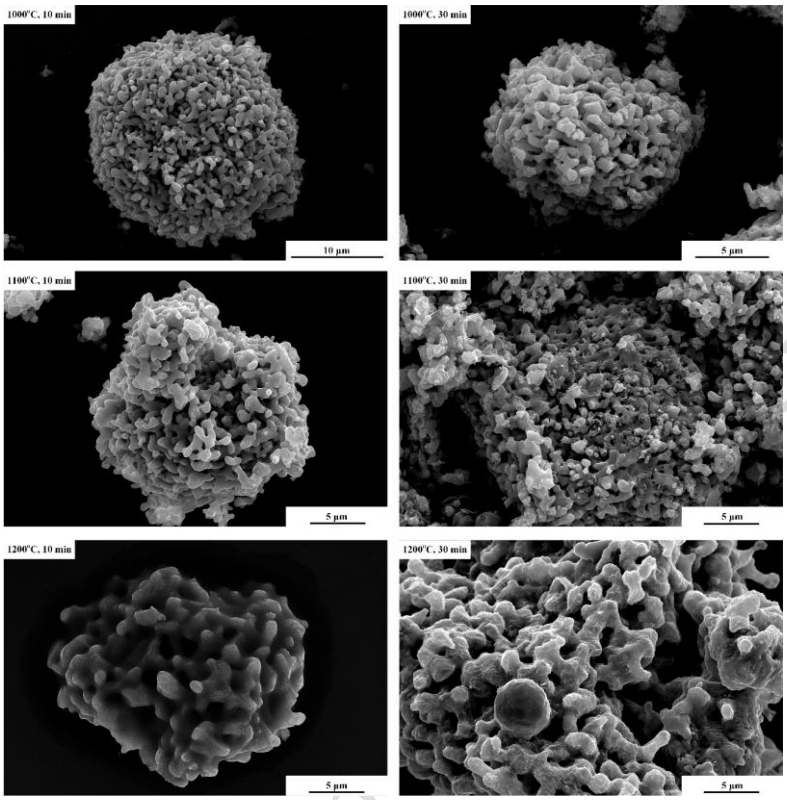

Figure 7 SEM images of the samples with 10 wt.% Fe_2O_3 additives reduced at three temperatures for different time.

3.2 Reduction degree and carbonitriding ratio

According to the content of titanium phase in each sample based on Rietveld refinement, the carbonitriding ratio (CR) and reduction degree (RD) of each sample can be calculated from equations (1) and (2):

$$CR = \frac{n_{TiC_xN_yO_Z}}{n_{Total\text{-}Ti}} = \frac{n_{TiC_xN_yO_Z}}{n_{Ti}}$$

$$RD = \frac{n_{loss\text{-}O}}{n_{Total\text{-}O}} = \frac{2n_{Ti} - 2n_{TiO_2} - \sum_{i=2}^{10}(2i-1)\cdot n_{Ti_iO_{2i-1}} - z\cdot n_{TiC_xN_yO_Z}}{2n_{Ti}} \quad (2)$$

where n_{Ti}, n_{TiO_2}, $n_{Ti_iO_{2i-1}}$ and $n_{TiC_xN_yO_Z}$ are the molar quantities of Ti atom, TiO_2, Ti_iO_{2i-1} and Ti(C, N, O), respectively; $n_{loss\text{-}O}$ is the lost molar quantity of O atom; $n_{Total\text{-}O}$ and $n_{Total\text{-}Ti}$ are the total molar quantities of O atom and Ti atom in TiO_2, respectively.

Figure 8 illustrates the relationship between the reduction degree, carbonitriding ratio, and the reaction time. It is evident that both the reduction degree and carbonitriding ratio increase as the reaction time is extended. This indicates a decrease in the oxygen content and an increase in the Ti(C, N, O) content as the reaction progresses, which aligns with the thermodynamic calculation results.

Comparing the results of reduction-carbonitriding at different temperatures, several observations can be made. Firstly, during the initial 10 minutes of reduction, the sample's reduction degree increases with the temperature: from 5.1% at 1000 ºC to 23.2% at 1100 ºC, and 29.4% at 1200 ºC. Additionally, the time required for complete carbonitriding decreases with increasing temperature: 40 minutes at 1100 ºC to 30 minutes at 1200 ºC. At 1000 ºC, the reaction degree and carbonitriding ratio are relatively low, resulting in the maximum reaction value not being reached even after 90 minutes of reaction. When the reaction temperature is raised to 1100°C, significant improvements are observed. The carbonitriding ratios for 10 minutes, 20 minutes, 30 minutes, and 40 minutes are 0.19, 0.55, 0.86, and 0.96 respectively, indicating that the carbonitriding reaction has been largely completed. However, due to the presence of a certain amount of oxygen in the Ti(C, N, O) solid solution, the maximum reduction degree reaches only 0.75. After 30 minutes of reaction at 1200 °C, the carbonitriding ratio of TiO_2 reaches 0.97, confirming that the reaction rate can be significantly improved by increasing the temperature. However, the maximum reduction degree achieved is 0.73, slightly lower than that at 1100 °C. This can be attributed to the increased temperature leading to the sintering of solid materials, which hinders gas transport within the solid. Meanwhile, increasing deposited carbon with increasing reduction time will adhere to the surface of the sample particles, which again hinders the internal diffusion of gases. Consequently, the titanium oxide in the particle core cannot be fully reduced and carbonitrided.

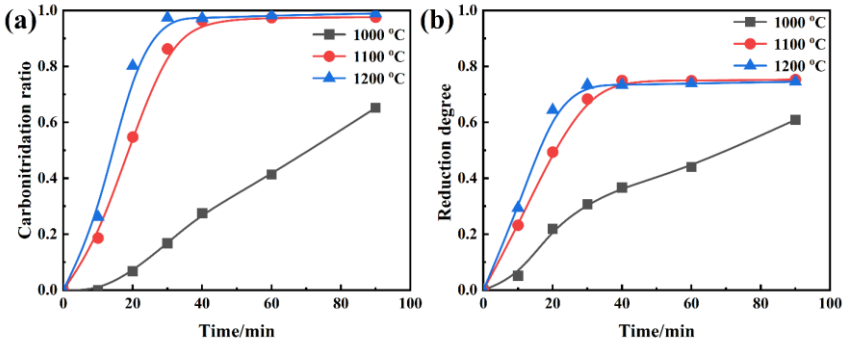

Figure 8 The relationship of (a) carbonitriding ratio and (b) reduction degree with the reaction time at different temperatures in CH_4-H_2-N_2 gas mixture

3.3 Reduction kinetics

Combined with our previous research results[2, 28], the reduction reaction of TiO_2 occurs from the surface of the powder to the inside of the powder. Therefore, the reduction process of TiO_2 in CH_4-H_2-N_2 gas mixture can be described by the unreacted core model. And the whole reaction process can be divided into the following steps:

1. CH_4, H_2 and N_2 molecules reach the gas phase boundary layer through the gas phase body;
2. Gas molecules reach the reaction interface through the porous product layer;
3. Physical adsorption of gas molecules at the reaction interface;
4. Dissociation and chemisorption of gas molecules at the reaction interface;

5. The adsorbed gas molecules react with the matrix at the reaction interface;
6. The gas products diffuse through the solid product layer;
7. The gas products pass through the gas phase boundary to the gas phase body.

Usually, the limiting steps of the unreacted core model includes three parts: external diffusion (steps 1 and 7), internal diffusion (steps 2 and 6) and interfacial chemical reaction (step 5). The external diffusion limit can generally be eliminated by increasing the gas flow rate. Therefore, interfacial chemical reaction or internal diffusion of gas is the most likely limiting step for gas-solid reactions in most cases. The experimental results indicate that the initial stage of reduction involved the reduction of iron oxide and the transformation of TiO_2 to a variety of low valent titanium oxides. This transformation follows the path of TiO_2 → Magnéli → Ti_3O_5 →Ti_2O_3 → Ti(N, C, O), and the carbonitrided reaction of TiO_2 can be described as follows:

$$TiO_2+(2+x-z)CH_4+0.5y\,N_2 \rightleftharpoons TiC_xN_yO_Z+(2-z)CO+(4+2x-2z)H_2 \quad (3)$$

The increase in temperature significantly accelerated the transition rate, suggesting that the interfacial chemical reaction was most likely to be the limiting step. And the internal diffusion of gas was most likely to be the limiting step at the late stage of reduction due to dense product layer and excessive deposition of carbon. The kinetic equations of chemical reaction and internal diffusion control in the unreacted core model are as follows[33, 34]:

$$1 - (1 - \alpha)^{1/3} = k_1 t \quad (4)$$

$$1 - 2/3\,\alpha - (1 - \alpha)^{2/3} = k_2 t \quad (5)$$

where α is the reaction fraction; k_1 and k_2 are the reaction rate constants; and t is the reaction time.

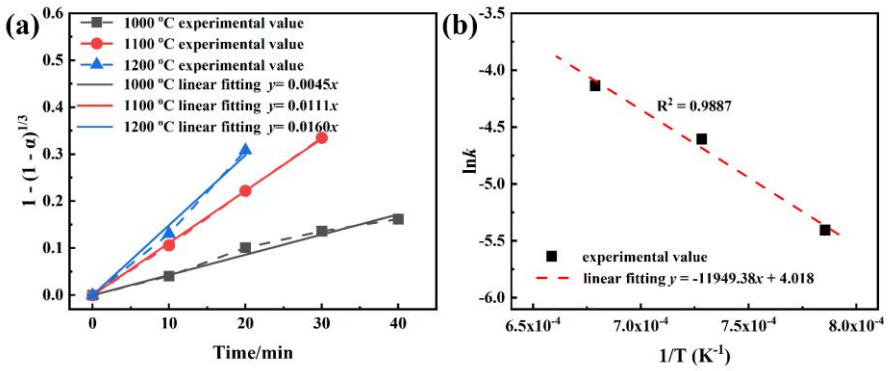

Figure 9 (a) Plots of reduction degree curve vs kinetic equation controlled by chemical reaction and (b) the Arrhenius plot for TiO_2 - 10 *wt.*% Fe_2O_3 samples reduced in CH_4-H_2-N_2 gas mixture

Equations (4) and (5) were utilized to fit the relationship between the reduction degree α and the reaction time t, using the data from **Figure 8**. The resulting fitting curve is depicted in **Figure 9a**. The rate constant k value at each temperature was determined from the slope of each fitting line in **Figure 9a**, and the corresponding fitting results are presented in **Table 4**. By comparing the goodness-of-fit results for the two cases of rate-controlling steps, it was observed that the equation $1-(1-\alpha)^{1/3}$ exhibited

the best linear relationship with time *t*. This finding indicates that the carbonitriding reduction of TiO_2 in the CH_4-H_2-N_2 system is primarily governed by chemical reaction. When the reaction rate constant *k* is known, the apparent activation energy E_a of the reaction can be calculated by using the Arrhenius equation:

$$\ln k = -\frac{E_a}{R}\cdot\frac{1}{T}+\ln A \tag{6}$$

Table 4 The summary of kinetic model fitting results for TiO_2 - 10 *wt.*% Fe_2O_3 samples reduced in CH_4-H_2-N_2 gas mixture

T	$1-(1-\alpha)^{1/3}$		$1-2/3\,\alpha-(1-\alpha)^{2/3}$	
	k_1	R^2	k_2	R^2
1000 ℃	0.0045	0.9784	0.0005	0.9514
1100 ℃	0.0111	0.9996	0.0025	0.9085
1200 ℃	0.0160	0.9911	0.0034	0.9454

In the formula, *lnk* is the natural logarithm of reaction rate constant; E_a is the apparent activation energy ($J\cdot mol^{-1}$); *A* is the pre-exponential factor; *R* is the gas constant (8.314×10-3 $kJ\cdot mol^{-1}\cdot K^{-1}$); and *T* is the reaction temperature (K).

The relationships between ln*k* and 1/*T* at 1000 ºC ~ 1200 ºC are shown in **Figure 9b**. The results show that there is a good linear relationship between ln*k* and 1/*T*: ln*k* =-11949.38/T+4.018, and the goodness of fit is 0.9887. The apparent activation energy of carbonitriding reduction of TiO_2 in CH_4-H_2-N_2 system is 99.35 kJ/mol.

4. Conclusions

In this study, the reduction degree and carbonitriding ratio of TiO_2 in the CH_4-H_2-N_2 system were investigated, and the kinetics of carbonitriding reduction were analyzed. The following conclusions can be drawn from the study:

(1) The reduction degree of the TiO_2 sample exhibited a notable increase as the temperature ranged from 1000 °C to 1200 °C. At the same time, the complete carbonitride time decreased with increasing temperature. However, it was observed that extremely high temperatures (1200 °C) can impact the reduction degree. Therefore, the optimal reduction temperature was determined to be 1100 °C, where a balance between reduction degree and reaction time was achieved.

(2) The carbonitriding reduction process of TiO_2 in the CH_4-H_2-N_2 system was found to follow the unreacted nuclear model, and it is primarily controlled by chemical reactions. The apparent activation energy of the carbonitriding reduction process was determined to be 99.35 kJ/mol.

Overall, these findings advance our understanding of the carbonitriding reduction kinetics of TiO_2 in the CH_4-H_2-N_2 system.

Acknowledgments

Thanks are given to the financial supports from the National Natural Science Foundation of China (52074057, 52222408), Chongqing Natural Science Foundation (cstc2021jcyj-msxmX0049), and the China Postdoctoral Science Foundation

(2023M730426).

Author contributions

R. Zhang performed the original draft writing and leaded the formal analysis. G. Fan conducted the writing-reviewing. Y. Hou and Y. You conducted the editing. Pro. J. Dang conducted the supervision and project administration.

Data availability

The data of this work could be obtained by contacting with the corresponding author by e-mail.

Conflict of interest

On behalf of all authors, the corresponding author states that there is no conflict of interest.

Reference

[1] Z.Z. Fang, S. Middlemas, J. Guo, P. Fan, A new, energy-efficient chemical pathway for extracting Ti metal from ti minerals, Journal of the American Chemical Society, 135(49) (2013) 18248. https://doi.org/10.1021/ja408118x

[2] R. Zhang, D. Liu, G.Q. Fan, H.B. Sun, J. Dang, Thermodynamic and experimental study on the reduction and carbonization of TiO_2 through gas-solid reaction, International Journal of Energy Research, 43(9) (2019) 4253-4263. https://doi.org/10.1002/er.4551

[3] K. Stanaway, Overview of Titanium Dioxide Feedstocks, Mining engineering, 46(12) (1994) 1367-1370.

[4] A. Rajabi, M.J. Ghazali, A.R. Daud, Chemical composition, microstructure and sintering temperature modifications on mechanical properties of TiC-based cermet – A review, Materials & Design, 67 (2015) 95-106. https://doi.org/10.1016/j.matdes.2014.10.081

[5] S.S. Zhao, X.H. Gao, X.L. Qiu, D.M. Yu, G.K. Tian, A novel TiC-TiN based spectrally selective absorbing coating: Structure, optical properties and thermal stability, Infrared Physics & Technology, 110 (2020) 103471. https://doi.org/10.1016/j.infrared.2020.103471

[6] B. Kilinç, E. Kocaman, S. Sen, U. Sen, Effect of titanium content on the microstructure and wear behavior of $Fe_{(13-x)}Ti_xB_7$ (x=0-5) hardfacing alloy, Journal of Mining and Metallurgy, Section B: Metallurgy, 58(1) (2022) 29-41. https://doi.org/10.2298/JMMB210430047K

[7] E. Ahmadi, R.O. Suzuki, T. Kikuchi, T. Kaneko, Y. Yashima, Towards a sustainable technology for production of extra-pure Ti metal: Electrolysis of sulfurized Ti(C,N) in molten $CaCl_2$, International Journal of Minerals, Metallurgy and Materials, 27(12) (2020) 1635-1643. https://doi.org/10.1007/s12613-020-2162-5

[8] Q.Y. Wang, Y. Li, S.Q. Jiao, H.M. Zhu, Producing metallic titanium through electro-refining of titanium nitride anode, Electrochemistry Communications, 35 (2013) 135-138. https://doi.org/10.1016/j.elecom.2013.07.047

[9] Q.Y. Wang, J.X. Song, J.Y. Wu, S.Q. Jiao, J.G. Hou, H.M. Zhu, A new consumable anode material of titanium oxycarbonitride for the USTB titanium process, Physical Chemistry Chemical Physics, 16(17) (2014) 8086-8091. https://doi.org/10.1039/C4CP00185K

[10] M. Ali, P. Basu, Mechanochemical synthesis of nano-structured TiC from TiO_2 powders, Journal of

Alloys and Compounds, 500(2) (2010) 220-223. https://doi.org/10.1016/j.jallcom.2010.04.007
[11] K.H. Wu, Y. Jiang, S.Q. Jiao, K.C. Chou, G.H. Zhang, Preparations of titanium nitride, titanium carbonitride and titanium carbide via a two-step carbothermic reduction method, Journal of Solid State Chemistry, 277 (2019) 793-803. https://doi.org/10.1016/j.jssc.2019.07.041
[12] Y.F. Yang, D.K. Mu, Rapid dehydrogenation of TiH_2 and its effect on formation mechanism of TiC during self-propagation high-temperature synthesis from TiH_2–C system, Powder Technology, 249 (2013) 208-211. https://doi.org/10.1016/j.powtec.2013.08.020
[13] C. Saringer, C. Kickinger, F. Munnik, C. Mitterer, N. Schalk, M. Tkadletz, Thermal expansion of magnetron sputtered TiC_xN_{1-x} coatings studied by high-temperature X-ray diffraction, Thin Solid Films, 688 (2019) 137307. https://doi.org/10.1016/j.tsf.2019.05.026
[14] J.G. Deng, M. Braun, I. Gudowska, Properties of TiCN coatings prepared by magnetron sputtering, Journal of Vacuum Science & Technology A, 12(3) (1994) 733-736. https://doi.org/10.1116/1.578815
[15] P.B. Mi, J.N. He, Y.F. Qin, K. Chen, Nanostructure reactive plasma sprayed TiCN coating, Surface and Coatings Technology, 309 (2017) 1-5. https://doi.org/10.1016/j.surfcoat.2016.11.033
[16] Z.P. Lv, W.S. Ma, M. Wang, J. Dang, K.L. Jian, D. Liu, D.J. Huang, Co-Constructing Interfaces of Multiheterostructure on MXene ($Ti_3C_2T_x$)-Modified 3D Self-Supporting Electrode for Ultraefficient Electrocatalytic HER in Alkaline Media, Advanced Functional Materials, 31(29) (2021) 2102576. https://doi.org/10.1002/adfm.202102576
[17] Z.P. Lv, M. Wang, D. Liu, K.L. Jian, R. Zhang, J. Dang, Synergetic Effect of Ni_2P and MXene Enhances Catalytic Activity in the Hydrogen Evolution Reaction, Inorganic Chemistry, 60(3) (2021) 1604-1611. https://doi.org/10.1021/acs.inorgchem.0c03072
[18] J. Tang, M.S. Chu, F. Li, C. Feng, Z.G. Liu, Y.S. Zhou, Development and progress on hydrogen metallurgy, International Journal of Minerals Metallurgy and Materials, 27(6) (2020) 713-723. https://doi.org/10.1007/s12613-020-2021-4
[19] B.B. Liu, Y.B. Zhang, Z.J. Su, Z.W. Peng, G.H. Li, T. Jiang, Thermodynamic Analysis and Reduction of MnO_2 by Methane–Hydrogen Gas Mixture, JOM, 69(9) (2017) 1669-1675. https://doi.org/10.1007/s11837-017-2456-x
[20] R. Alizadeh, E. Jamshidi, H. Ale Ebrahim, Kinetic study of nickel oxide reduction by methane, Chemical Engineering & Technology, 30(8) (2010) 1123-1128. https://doi.org/10.1002/ceat.200700067
[21] O. Ostrovski, G.Q. Zhang, Reduction and carburization of metal oxides by methane-containing gas, Aiche Journal, 52(1) (2010) 300-310. https://doi.org/10.1002/aic.10628
[22] T. Leino, P. Taskinen, R.H. Eric, Determination of Metallization Degree of Pre-reduced Chromite with Image and Rietveld Analysis, Journal of Mining and Metallurgy, Section B: Metallurgy, 56(3) (2020) 289-297. https://doi.org/10.2298/JMMB200313022L
[23] G.Q. Zhang, O. Ostrovski, Reduction of titania by methane-hydrogen-argon gas mixture, Metallurgical and Materials Transactions B, 31(1) (2000) 129-139. https://doi.org/10.1007/s11663-000-0138-4
[24] G.Q. Zhang, O. Ostrovski, Reduction of ilmenite concentrates by methane-containing gas: Part I. Effects of ilmenite composition, temperature and gas composition, Canadian Metallurgical Quarterly, 40(3) (2001) 317-326. https://doi.org/10.1179/cmq.2001.40.3.317
[25] J. Dang, F. Fatollahi Fard, P.C. Pistorius, K.C. Chou, Synthesis of Titanium Oxycarbide from Concentrates of Natural Ilmenite (Weathered and Unweathered) and Natural Rutile, Using a Methane-Hydrogen Gas Mixture, Metallurgical & Materials Transactions B, 48 (2017) 2440–2446. https://doi.org/10.1007/s11663-017-1048-z

[26] J. Dang, F. Fatollahi Fard, P.C. Pistorius, K.C. Chou, Synthesis of titanium oxycarbide from titanium slag by methane-containing gas, Metallurgical and Materials Transactions B, 49(1) (2018) 123-131. https://doi.org/10.1007/s11663-017-1123-5

[27] R. Zhang, J. Dang, D. Liu, Z.P. Lv, G.Q. Fan, L.W. Hu, Reduction of perovskite-geikielite by methane–hydrogen gas mixture: Thermodynamic analysis and experimental results, Science of The Total Environment, 699 (2020) 134355. https://doi.org/10.1016/j.scitotenv.2019.134355

[28] G.Q. Fan, Y.L. Hou, D.J. Huang, J. Dang, R. Zhang, J.Y. Xiang, X.W. Lv, X.M. Ding, Synthesis of Ti(C, N, O) ceramic from rutile at low temperature by CH_4-H_2-N_2 gas mixture, International Journal of Refractory Metals and Hard Materials, 101 (2021) 105659. https://doi.org/10.1016/j.ijrmhm.2021.105659

[29] G.Q. Fan, M. Wang, J. Dang, R. Zhang, Z.P. Lv, W.C. He, X.W. Lv, A novel recycling approach for efficient extraction of titanium from high-titanium-bearing blast furnace slag, Waste Management, 120 (2021) 626-634. https://doi.org/10.1016/j.wasman.2020.10.024

[30] M.A. Ermakova, D.Y. Ermakov, A.L. Chuvilin, G.G. Kuvshinov, Decomposition of methane over iron catalysts at the range of moderate temperatures: The influence of structure of the catalytic systems and the reaction conditions on the yield of carbon and morphology of carbon filaments, Journal of Catalysis, 201(2) (2001) 183-197.

[31] J. Hua, K. Wei, Q. Zheng, X. Lin, Influence of calcination temperature on the structure and catalytic performance of Au/iron oxide catalysts for water–gas shift reaction, Applied Catalysis A General, 259(1) (2004) 121-130.

[32] N. Bost, M.R. Ammar, M.L. Bouchetou, J. Poirier, The catalytic effect of iron oxides on the formation of nano-carbon by the Boudouard reaction in refractories, Journal of the European Ceramic Society, 36(8) (2016) 2133-2142.

[33] C.Y. Lu, X.L. Zou, X.G. Lu, X.L. Xie, K. Zheng, W. Xiao, H.W. Cheng, G.S. Li, Reductive kinetics of Panzhihua ilmenite with hydrogen, Transactions of Nonferrous Metals Society of China, 26(12) (2016) 3266-3273. https://doi.org/10.1016/S1003-6326(16)64460-6

[34] X.G. Si, X.G. Lu, C.W. Li, C.H. Li, W.Z. Ding, Phase transformation and reduction kinetics during the hydrogen reduction of ilmenite concentrate, International Journal of Minerals, Metallurgy, and Materials, 19(5) (2012) 384-390. https://doi.org/10.1007/s12613-012-0568-4